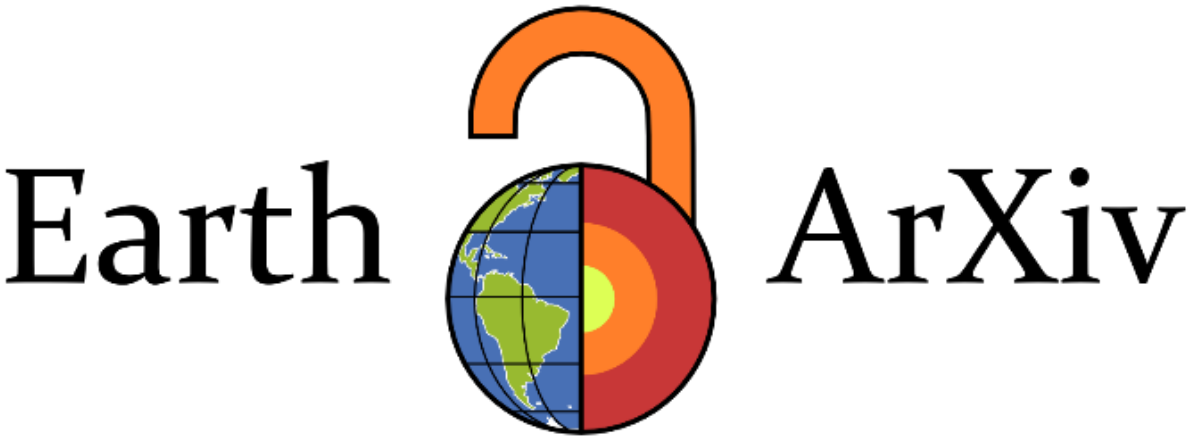

Machine learning estimates for G20 subnational GHG emissions from 2000-2020 using self-reported emissions data

Ying Yu[1,2†], Xuewei Wang[1,2†], Diego Manya[1†] and Angel Hsu[1,2*]
[1] Data-Driven EnviroLab, UNC Institute for the Environment, University of North Carolina at Chapel Hill
[2] Department of Public Policy, University of North Carolina at Chapel Hill

† Authors contributed equally and are co-first authors
* Corresponding author: Angel Hsu (angel.hsu@unc.edu)

Abstract

Reliable, comparable greenhouse gas (GHG) emissions data at the subnational level remain scarce, despite growing expectations for cities and regions to lead on climate action. Inconsistent reporting, methodological variation, and limited coverage of self-reported inventories hinder efforts to track progress and guide mitigation opportunities. To address these challenges, we develop a machine learning (ML) framework to estimate annual Scope 1 and 2 CO_2-equivalent emissions for subnational jurisdictions in G20 countries from 2000 to 2020. Our approach integrates publicly available geospatial, socioeconomic, and environmental data with self-reported inventories where available, and aligns predictions with subnational administrative boundaries. Compared to traditional downscaling or proxy-based approaches, our model improves spatial relevance and predictive performance while capturing locally specific emission drivers. This globally consistent, administratively-aligned dataset can serve as a baseline for assessing climate progress, especially in data-poor or inconsistent reporting contexts, and supports more targeted, data-informed policy decisions for urban and regional decarbonization.

Background & Summary

More than 14,000 city and regional governments have pledged climate actions under various voluntary initiatives.[1] These local actors often submit climate action plans, which include emission reduction pledges and related commitments to more than 30 transnational subnational government-focused transnational initiatives, as tracked by the UN Framework Convention on Climate Change (UNFCCC) Non-State Actor Zone for Climate Action (NAZCA). Nearly 300 large cities over 500,000 in population[2] and 570 cities and regions in the G-20 have even pledged net-zero targets.[3] Yet despite their growing visibility in global climate governance, fewer than 10 percent have reported greenhouse gas emission (GHG) inventories to track their progress over time.[3] When emissions are reported, they are frequently incomparable due to methodological differences, self-selection of emission sources included, treatment of consumption-based or "out-of-boundary" emissions, among others.[4–6] This gap, between signalled intent and accountability,

underscores a critical challenge: while cities and regions are increasingly seen as key players in advancing both local and global climate goals, the absence of consistent, high-quality emissions data limits our ability to evaluate their impact and guide future investments in needed decarbonization efforts.

To address challenges related to data gaps, accounting inconsistencies, and comparability across scales, researchers have adopted a range of methods. These include statistical downscaling of national emissions data to the subnational level,[7–12] as well as activity-based spatial allocation approaches that use sector- and activity-specific proxies, such as the locations of power plants, industrial facilities, or patterns of residential and agricultural emissions. These proxy-driven methods often rely on geospatial datasets such as the Emissions Database for Global Atmospheric Research (EDGAR) or the Open-source Data Inventory for Anthropogenic CO_2 (ODIAC) datasets, which utilize satellite remote sensing and other geospatial data as proxies, to allocate emissions within countries at finer spatial resolutions. However, these existing approaches suffer from several shortcomings. Statistically-downscaled city-level datasets fail to adequately capture the impact of subnational climate efforts since these methodologies assume that cities follow national-level trajectories of coarse GHG emission proxies like GDP and population, drowning out any potential signal of mitigation progress. Large gridded, geospatial datasets have the advantage of providing consistent assessment methodology, complete spatial and temporal resolution, and comparability. However, they are not aligned with city administrative and decision-making boundaries, limiting their utility and application to understanding subnational climate action progress. These approaches tend to have overall lower prediction accuracy and modeling limitations, particularly for complex urban scenarios and broader generalizability is also questionable.[13]

The rapid advancement of artificial intelligence (AI), particularly machine learning (ML) techniques, has opened up new opportunities for addressing persistent data and analytical challenges in climate science. One of the most promising applications of ML is its ability to help fill critical data gaps, since ML methods excel at integrating large, heterogeneous datasets and identifying complex, non-linear relationships between key drivers of emissions, such as energy consumption, industrial activity, land use, and socio-economic indicators.[14–16] These approaches have the potential to significantly improve over traditional subnational GHG estimation approaches by leveraging a more flexible approach where algorithms “learn” complex patterns in the data without relying on predefined assumptions.[13] Particularly for large, heterogeneous datasets, ML approaches could enable a more comprehensive and dynamic understanding of urban environments and emissions.[13] For example, Hsu et al. (2022)[17] utilized a gradient-boosting “tree model” ML framework (XGBoost)[18] and underlying satellite remote-sensing derived geospatial predictors to estimate likely annual emissions and mitigation performance of all local administrative areas in Europe between 2001 and 2018. Neural networks and deep learning frameworks are also being introduced for prediction.[19]

Generalizing a global ML-based approach to cities across the world has its challenges. Globally, cities are diverse across a range of variables. They differ greatly in their physical morphology, such as urban form, land use patterns, and infrastructure, which directly influence the spatial distribution and magnitude of emissions.[20] Variations in economic development levels further complicate modeling, as cities in high-income regions often have distinct energy systems, transportation networks, and building codes compared to those in low- and middle-income countries. Moreover, cities span a wide range of population sizes, densities, and geographic extents, each of which affects emission sources and intensities in unique ways. The mix of emission sources, ranging from heavy industry and power generation to informal settlements and biomass use, also varies significantly, requiring models to account for locally specific drivers and activities. As a result, ML models trained on data from one set of cities may not generalize well to others unless they are carefully calibrated, incorporate locally relevant variables, and leverage multi-source data to capture these differences.

To address these limitations, the dataset we introduce in this paper develops a machine learning framework to predict urban greenhouse gas emissions for subnational governments in G20 countries from 2000-2020. Our approach leverages a wide array of publicly available geospatial, socioeconomic, and environmental data, integrating these with self-reported emissions inventories from cities wherever available. A key distinguishing feature of our methodology is the use of the Global Administrative Areas Database (GADM) v.4.1,[21] which provides a globally consistent hierarchy of administrative boundaries. By aligning emission estimates with officially recognized city and municipal governance units, this approach enhances the relevance and usability of the data for local decision-makers. Unlike traditional statistical downscaling methods or other proxy-based geospatial modeling approaches, which often assume that urban emissions follow national-level trends and thus fail to capture local mitigation actions or unique city characteristics, our ML model is designed to extract additional, non-linear insights from diverse data sources, improving both the completeness and accuracy of city-level emissions estimates. While this dataset is not intended to replace cities' own greenhouse gas inventories, we aim for it to serve as a comparable, globally consistent baseline that can support cities in tracking progress, identifying gaps, and informing climate action planning, particularly in contexts where self-reported data are unavailable, inconsistent, or outdated and when other gridded products underestimate emissions in smaller subnational entities.

Method

Workflow

The dataset workflow of this study is illustrated in Figure 1. It starts with the cleaning and standardization of self-reported emissions data, followed by the spatial alignment of subnational actors. Then we extracted environmental predictor variables from 2000 to 2020 for all

subnational administrative units in the scope of this study. We conducted data validation and quality checks before model training and implementation. Finally, we compared predicted emissions with external datasets. Each of these steps is described in the following sections.

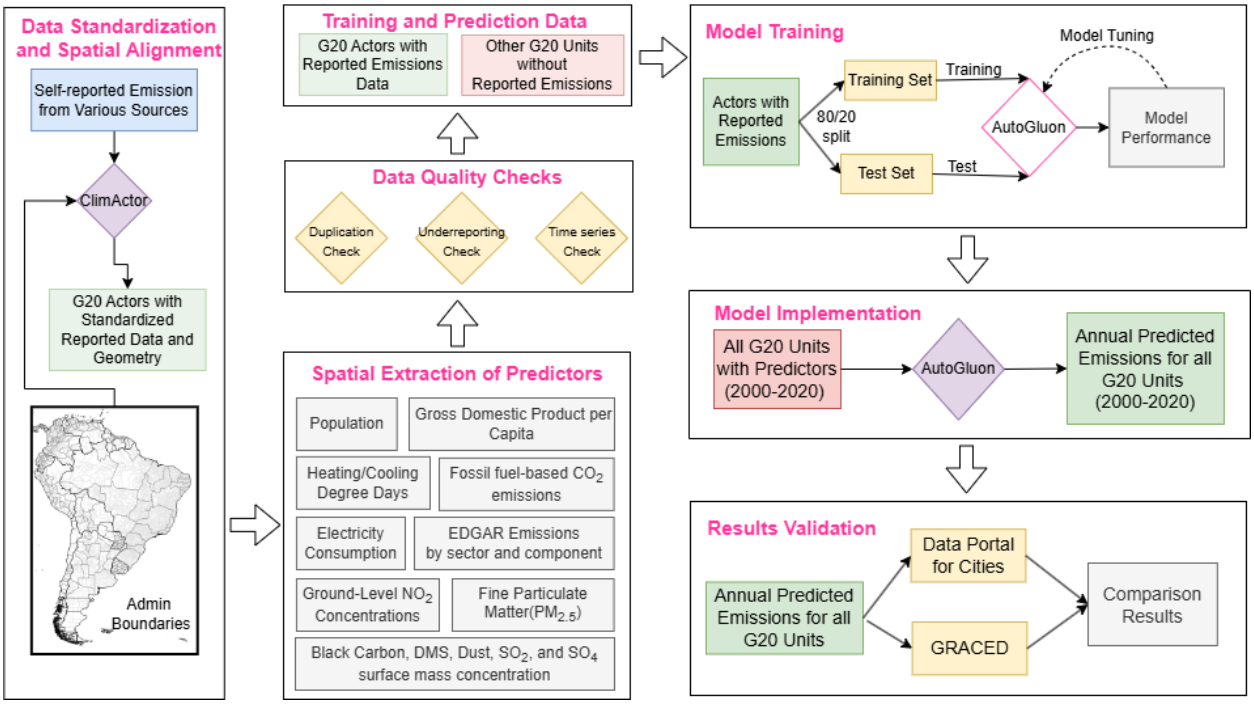

Figure 1. Workflow diagram of data processing, model training, and validation.

Study Area

Our study focuses on the G20 (the European Union, Argentina, Australia, Brazil, Canada, China, France, Germany, India, Indonesia, Italy, Japan, South Korea, Mexico, Russia, Saudi Arabia, South Africa, Turkey, the United Kingdom, and the United States), which collectively comprise nearly 80% of global greenhouse gas emissions.[22] We include subnational entities across all administrative levels with available data that met quality controls, excluding only the highest administrative units (i.e., Regions), unless they were classified at least 50% urban based on the urban-rural classification from Yu et al. (2025).[12] The final dataset included 5,972 cities and 116 regions in the G20 and a total of 9,664 self-reported emissions entries for several years, with 2,273 entities reporting emissions more than once. Figure 2 shows the geographical distribution and type of subnational entities included in our final training dataset.

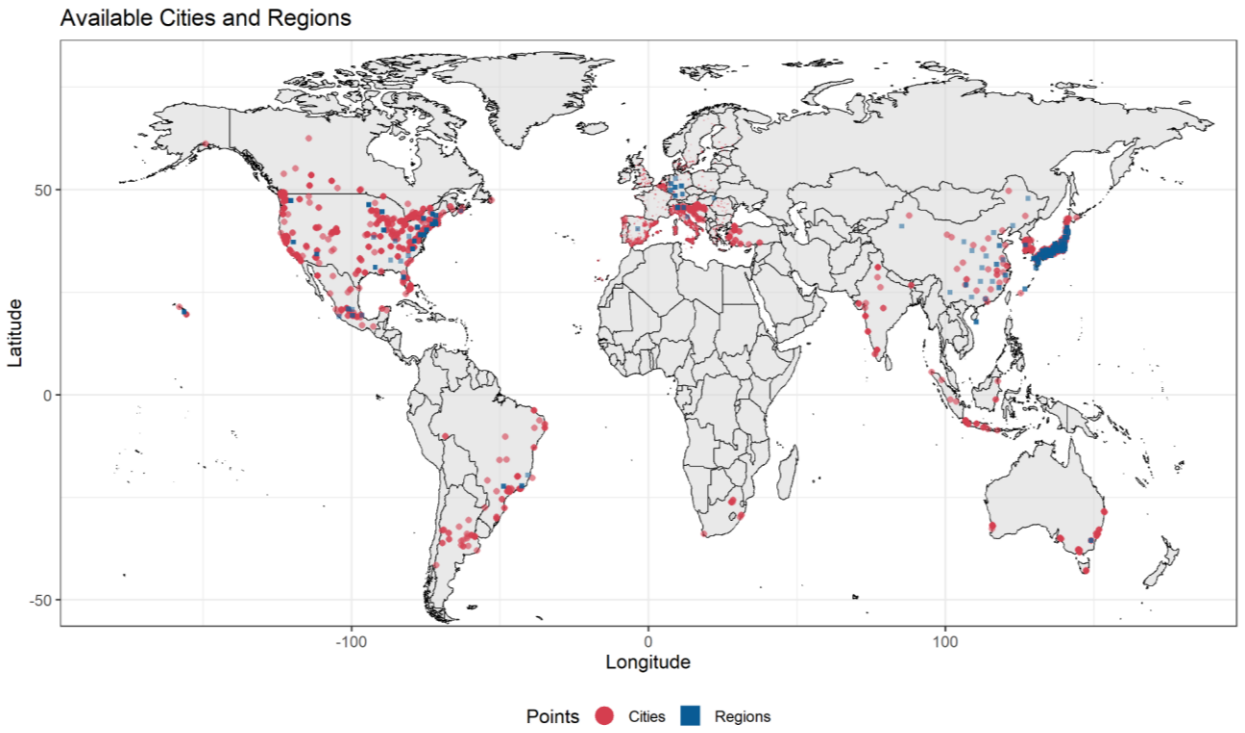

Figure 2. Map of cities (n=5,972) and regions (n=116) with self-reported emissions used to train and test our machine learning model.

While not representative of all subnational jurisdictions globally, the entities included in our dataset offer a revealing snapshot of those that have voluntarily self-reported their greenhouse gas emissions, which tend to be more likely located in more resource-rich areas such as Europe and North America. The majority of reporting entities in our training dataset are from Europe, followed by North America and East Asia and the Pacific (see Table 1 for summary statistics). Among these, reporting entities in Europe tend to have the smallest administrative territories and the lowest populations, representing the lowest average self-reported emissions. Notably, this region has the second-highest average GDP per capita. Reporting entities in North America have the highest average GDP per capita and the third-highest average emissions. Those from East Asia and the Pacific report the second highest emission values amongst all regions, but have the highest average population and administrative area. In Latin America and the Caribbean, our dataset includes reporting entities from Argentina, Brazil, and Mexico. They have administrative territories similar in size to those in North America, but, on average, have twice the population and lower emissions. In Eastern Europe and Central Asia, reporting entities are limited to just two countries: 46 from Croatia and 16 from Turkey. Croatian entities resemble their western European counterparts, with smaller populations, lower self-reported emissions, and smaller administrative areas. Turkish entities, by contrast, are far larger in population, averaging 100 times more than those from Croatia, and report more than 5 million tons of CO_2 annually. In South Asia, our dataset only includes reporting cities and regions from Indonesia, which have relatively low GDP per capita but substantial average emissions, suggesting high-emitting local

activities amid slower economic development. Finally, due to limited self-reported data, Sub-Saharan Africa is only represented by a small number of entities, all of which are major cities: Johannesburg, Ekurhuleni, Tshwane, KwaDukuza, Cape Town, and eThekwini.

Table 1. Summary of reporting entities in training data.

Region	Entities (n)	Self-reported Emission Data Points	Average Population	Average GDP Per capita (standardized to 2021 international US dollars)	Average Emissions (tons CO_2 e)	Administrative Area (km^2)
Europe	5,313	7,975	47,466 (±450,297)	39,905.09 (±12,209.67)	338,611.2 (±4,505,677.97)	217.01 (±2,367.97)
North America	323	824	991,624 (±3,279,134)	61,826.16 (±22,305.76)	12,454,455.87 (±37,069,396.64)	12,626.87 (±53,209.97)
East Asia and the Pacific	280	575	5,368,728 (±16,193,127)	33,549.78 (±15,506.36)	39,778,130.81 (±121,421,800.8)	21,642.65 (±110,260.03)
Latin America and Caribbean	86	151	2,078,074 (±563,8822)	18,602.95 (±10,217.11)	9,825,536.59 (±23,618,735.85)	12,139 (±38,168.77)
Eastern Europe and Central Asia	62	97	553,345 (±1,946,072)	20,419.64 (±8,514.42)	2,431,632.42 (±7,398,410.31)	1,984.12 (±4,576.56)
South Asia	12	32	2,909,023 (±5,339,328)	10,495.21 (±4,295.22)	9,089,828.51 (±19,602,242.65)	214.57 (±378.64)
Sub-Saharan Africa	6	10	3,654,199 (±1,828,698)	15,741.19 (±4,358.23)	48,841,156.5 (±28,994,336.29)	2,919.85 (±2,136.73)

Self-reported CO_2 Emissions

We use a broad definition of subnational actors to include any subnational entity with jurisdiction over an administrative area, regardless of their denomination, or level of autonomy. To standardize geographic units across countries, we rely on a dataset built from the Global Administrative Areas Database (GADM) version 4.1[21] enhanced with more recent official boundaries for 17 countries with outdated boundary data, which organizes subnational areas according to each country's internal administrative hierarchy. In this system, administrative level 1 (ADM_1) represents the highest subnational division, and ADM_5 represents the lowest available level for any given country. Because national administrative structures vary, a unit such as a "Municipality" may appear at ADM_2 in one country and ADM_3 in another, depending on how that country's governance system is organized.

Examples of subnational entities in our dataset span a range of types, including provinces, states, counties, regions, districts, municipalities, and villages, with names varying by country and language. At the ADM_1 level, the top-tier subnational unit, common designations include Provinces (e.g., Argentina, Canada, China, Turkey, South Africa), States (e.g., Australia, Brazil, Germany, United States), and Regions (e.g., Belgium, Finland, France, Greece). ADM_1 also includes Counties (e.g., Estonia and Sweden) and Federal Districts (e.g., Argentina and Brazil). At the ADM_2 level, commonly used terms include Districts (e.g., Austria, Germany, Turkey), Municipalities (e.g., Brazil, Finland, Mexico), Cities (e.g., China, Indonesia, Japan), and Counties (e.g., United States). At the ADM_3 level, Municipalities remain the most dominant unit in countries such as Austria, Italy, and Poland, alongside similar structures like Communes (Luxembourg and Romania). Administrative units at ADM_4 units are less common but still present, for example Communes in Belgium, Cantons in France, and Municipalities in Spain. Supplementary Figure S1 provides a summary of the GADM levels by country for the reporting and predicted entities in our dataset.

From this broad definition, we collected open-sourced information for subnationals actors participating in national or international climate action networks and reporting platforms between 2019 and 2024, including: the Joint Research Centre (JRC), Global Covenant of Mayors and Energy (GCOM), EU Covenant of Mayors, Carbon Disclosure Project (CDP), C40 Cities for Climate Leadership Group, Japanese Ministry of the Environment, Local Governments for Sustainability (ICLEI) Carbonn® Climate Registry, Net Zero Tracker, Under2 Coalition, China Carbon Neutrality Tracker (CCNT), US Climate Mayors, US Climate Alliance, We Are Still In and the Global Climate Action Portal (GCAP or now renamed the Non-State Actor Zone for Climate Action or NAZCA) (see Online-only Table 2 for complete data source information and references). The collection process was performed either through direct access to the source's database, or indirect collection using HTML parsing tools such as BeautifulSoup v4.12.3. Online-only Table 2 lists the data sources used to compile the self-reported emissions data.

Once collected the data was transformed through two complementary processing steps: spatial alignment, to match each subnational reporting entity to its corresponding physical or administrative boundary, and standardization, to ensure consistency of actors' data reported across different platforms. The first step included extensive use and improvements to the ClimActor R package,[23] including improvements to the matching dictionary, the matching functions for automatic and machine-aided harmonization, and updates to the naming convention for subnational entities. The updated package, to be described and released in an upcoming publication, allowed us to consider not only nominal (i.e., name) matching but also our database of administrative boundaries. This process allowed us to attribute the self-reported climate information to policy relevant entities (i.e., local governments) and to leverage spatially-explicit data (e.g., remote sensing initiatives such as EDGAR to evaluate emissions data at multiple levels of governance. For the purposes of standardization we classified the highest administrative level (ADM_1) as "Regions," the next level down as (ADM_2) as 'Sub-Regions' and the remaining levels (ADM_3, ADM_4 and ADM_5) as "Cities."

The second stage involved a comprehensive cleaning and standardization of climate-related records for each entity, aimed at producing a consistent, structured database for each data source. The specific steps in this process varied depending on the origin of the data, as climate information was reported through diverse formats, including questionnaire responses, online dashboards, and downloadable databases. Each required tailored processing methods depending on which variables were collected. The process also included internal-consistency checks and ad-hoc fixes to the values to correct for identified errors commonly found in self-reported climate data, such as emissions units differences or misplaced data records. To enable systematic comparison and robust analysis across actors and platforms, when multiple GHG gases were individually reported, we standardized all emission values and targets into carbon dioxide equivalent (CO_2eq) using 100-year Global Warming Potential (GWP-100) values, consistent with those employed in the Intergovernmental Panel on Climate Change (IPCC) assessment reports.[24] Once each individual data source is harmonized we integrate all spatialized climate records into a single database consisting of a total of 24,084 records.

Several steps of data quality checks and data filtering methods were implemented. First, we filtered out duplicate emissions data, identified as multiple emission values from different initiatives collected for the same entities in the same reporting year. For instance, European cities participating in the Global Covenant of Mayors for Climate and Energy - EU Secretariat (EUCoM) directly report baseline and monitoring emissions inventories to the EU Joint Research Commission, which serves as the EUCoM Secretariat. The EU JRC regularly evaluates and validates the self-reported data and inventories, which involves assessing the data's completeness (according to their reporting criteria), coherence, and treatment of any outliers.[25] In 2021, the EU JRC published the first harmonized dataset for 6,200 EUCoM participants spanning 10 years of collected data. Since we regularly collected self-reported data points from the EUCoM website

starting from 2018,[26] we prioritized data for reporting entities from Kona et al. (2021)[25] since they had undergone an intensive evaluation and validation exercise. In other cases of duplicated emissions data, we kept only the highest total emissions value to avoid underreporting. Second, we calculated per capita emissions and excluded entries with implausible values outside the range of 0.02 to 80 tons per capita. The upper bound of 80 tons CO_2 per capita is informed by historical data from Qatar, which has the highest per capita emissions globally. While it peaked at 93.8 tons per capita between 1990 to 2023, most annual values are below 80 tons CO_2 per capita.[27] The lower bound of 0.02 tons CO_2 per capita is set just below the lowest value in this dataset, which is observed in Federated States of Micronesia and the Marshall Islands (0.04 to 0.05 tons CO_2 per capita). This threshold sets a reasonable buffer to include plausible emission per capita values while excluding any errors due to misreporting. Third, for entities reporting emissions in multiple years, we visually examined time series plots and removed outliers showing abrupt spikes or drops that suggested reporting error. Finally, after training our preliminary model and generating predicted emissions, we reviewed actors with predicted percentage error greater than one standard deviation from the mean by manually comparing and cross-checking reported emissions with other data sources to correct or remove data with potential reporting errors.

Comparison of self-reported inventories to globally-gridded emission products

To illustrate some of the challenges that arise when utilizing globally-gridded datasets to understand subnational climate action, Figure 3 shows a comparison of the records of self-reported subnational greenhouse gas inventories data against the widely-used EDGAR gridded dataset for a selection of the most commonly- reported sectors by cities (e.g., buildings, energy, industry, waste and ground transportation). As observed, gridded territorial emissions show a high correlation with self-reported inventories ($R^2 > 0.9$) at larger administrative areas such as states and regions (ADM_1). However, this correlation weakens at finer scales, where emissions are often systematically underestimated. These differences stem from several sources, including the limited spatial resolution of globally gridded datasets like EDGAR, differences in how emissions are allocated at the local level, and the challenge of capturing locally-specific activity data. For instance, gridded datasets often assign emissions to the location where they physically occur, such as a powerplant or landfill, rather to the location where electricity is consumed or waste is generated. In contrast, self-report emissions inventories more often account for these indirect or distributed emission sources, leading to higher reported inventory values. These attribution and granularity issues underscore the importance of aligning methodological assumptions when integrating global and local emissions data.

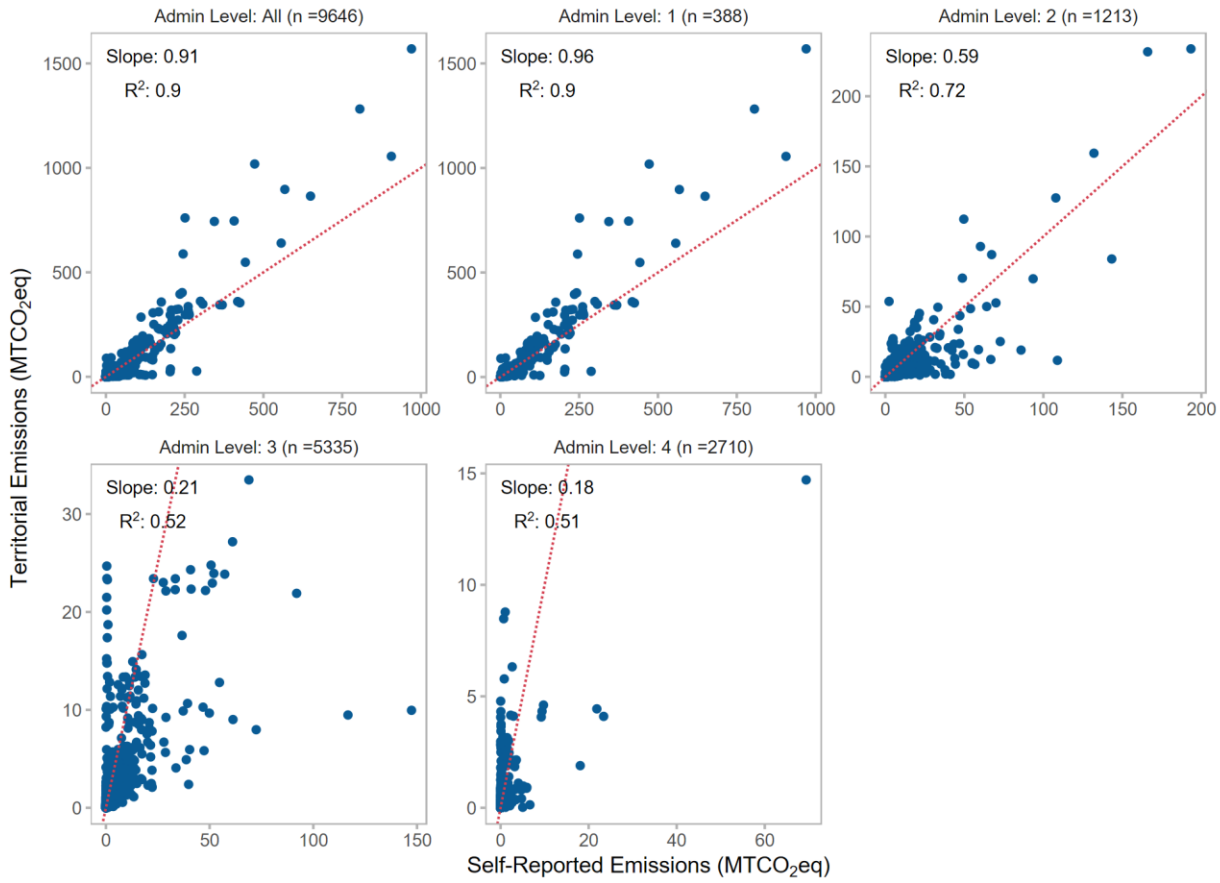

Figure 3. Comparison between self-reported subnational greenhouse gas emissions inventory data vs EDGAR territorial emissions for urban relevant sectors (e.g., buildings, energy, industry, waste and ground transportation).

Feature Selection

A critical step in our modeling framework is the identification of key predictors of city-level self-reported CO_2 emissions. Building on the machine learning framework developed by Hsu et al. (2022)[17] for predicting emissions and evaluating abatement performance in European cities, we draw from the existing literature on urban emission sources and drivers to construct a globally applicable set of predictors.[5,13,14,16]

To capture historical emission trends and their alignment with self-reported inventories, we incorporate annual fossil fuel CO_2 emissions from the Open-source Data Inventory for Anthropogenic CO_2 (ODIAC), which provides globally gridded data (2000–2023, 1 km × 1 km) on emissions from fossil fuel combustion, cement production, and natural gas flaring.[28] Additionally, we utilize the Emissions Database for Global Atmospheric Research (EDGAR v8.0 GHG), which provides sector-specific, gridded emissions of CO_2, CH_4, and N_2O from 1970 to 2022 at a 0.1° resolution. We focus on fossil-based sources, including combustion, industrial

processes (e.g., metal and mineral production), solvent use, and agricultural activities.[7] These sectoral emission data are consolidated into six main IPCC-based categories: transport, industry, agriculture, energy, buildings, and waste. CH_4 and N_2O emissions are processed similarly.

Recognizing that urban CO_2 emissions are not solely driven by stationary fossil fuel sources, we incorporate additional environmental indicators as proxies. Building on our previous study,[17] we included temperature-driven energy demand indicators such as heating and cooling degree days (HDD and CDD) calculated with the monthly NASA MERRA-2 temperature product from 2000 to 2020 (Bosilovich et al., 2015). The HDD and CDD are measured as the total temperature deviation from the reference temperature (T_{base}) (see equations 1-2 below), which is 15.5 °C for HDD and 22°C for CDD.[29] To better capture variation across regions and address the issue of zero CDD values observed in many European areas, we created a new variable, Temperature Difference, defined as the sum of CDD and HDD. This variable reflects the total number of degree days during which temperatures deviate from the baseline, whether due to heat or cold.

$$HDD = \Sigma_m(T_{base} - T_i) \times Days_m{}^{+} \text{ (Equation 1)}$$
$$CDD = \Sigma_m(T_i - T_{base}) \times Days_m{}^{+} \text{ (Equation 2)}$$

Air pollution, particularly nitrogen dioxide (NO_2) and fine particulate matter ($PM_{2.5}$) are often co-emitted with greenhouse gases, especially from fossil fuel combustion processes and transportation sources.[30] We included global satellite-derived $PM_{2.5}$ data from 2000 to 2020 at a $0.01° \times 0.01°$ resolution developed by the Atmospheric Composition Analysis Group[31,32] and the annual ground-level NO_2 concentrations from 2005 to 2019 at approximately 1 km resolution from the same research group.[33] We further applied linear extrapolation to the NO_2 data at the administrative unit level to fill gaps between the original dataset coverage and the scope of our study for years from 2000 to 2005 and 2020. Dust surface mass concentration (DUSMASS), black carbon surface mass concentration (BCSMASS), sulfur dioxide surface mass concentration (SO2SMASS), and sulfate surface mass concentration (SO4SMASS) are also included in our analysis from the MERRA-2 Monthly Mean Aerosol Diagnostics, Version 5.12.4 from 2000 to 2020.[34] Black carbon and sulfur oxides (SOx) are closely associated with energy use intensity and fossil fuel combustion.[35] While dust can originate from human activities and land cover and land use changes, these may also contribute to increased CO_2 emissions.[36]

We also processed gridded electricity consumption, population, and gross domestic product (GDP) as key socio-economic drivers of urban emissions. These variables are derived from Chen et al.[37] (electricity consumption, 1992–2019, 1 km), Schiavina et al.[38] (population, 1975–2030, 100 m), and Kummu et al.[39] (GDP, 1992–2022, 30 arc-seconds), respectively.

To generate the environmental variables used for model prediction, we applied zonal statistics to each administrative unit included in the study. This analysis was conducted across two platforms.

Variables such as population, GDP, electricity consumption, and emissions from EDGAR were processed using the ReduceRegion function in Google Earth Engine (GEE). In parallel, other spatial datasets, including ODIAC emissions, weather data, and air pollution metrics ($PM_{2.5}$, NO_2, dust, and SO_x), were processed using the *rasterstats* Python package version 0.15.0.[40] Depending on the nature of each variable, either the mean or the sum within each administrative boundary was calculated (see Table S1 for more details).

Model Specification

Since subnational CO_2 emissions are shaped by a complex non-linear, interdependent interaction of environmental, energy-related and socioeconomic factors, we employ AutoGluon, an automated machine learning (AutoML) framework that integrates various models, including deep neural networks, into a hierarchical ensemble.[41] AutoGluon automatically manages cross-validation, out-of-fold prediction tracking, and data shuffling, collectively mitigating overfitting and improving generalization.[42]

Given the heterogeneity of our input dataset, which includes variables collected at different spatial resolutions and temporal frequencies, AutoGluon is well suited for managing multi-source, scale-inconsistent features. For training and testing, we compile features from multiple sources, such as remote sensing satellites, ground-based monitoring, model-derived estimates, and statistical reports, including socioeconomic indicators, satellite-derived emission proxies, climate variables, and environmental pollution metrics. We allocate 80% of the full dataset to training, determined by a standard 80/20 random split, with the remaining 20% reserved for testing and validation.

Figure 4 below presents the feature importance plot (Figure 4a) and model performance based on the test dataset (Figure 4b). Overall, the predictive model demonstrates strong predictive capability, with a coefficient of determination (R^2) of 0.77 and a Mean Absolute Percentage Error (MAPE) of 38.57%, both calculated using the original (non-log-transformed) emission values. To facilitate visualization, we display the predicted emissions versus true emissions on a logarithmic scale. The feature importance table reports the relative contribution of each predictor to the model's overall predictive performance, among which population and GDP are the most important features, jointly accounting for approximately 50% of the model's explained variance. Additional contributors include CO_2 emissions from the building sector, electricity consumption, and longitude, which together explain another 10% of the variance.

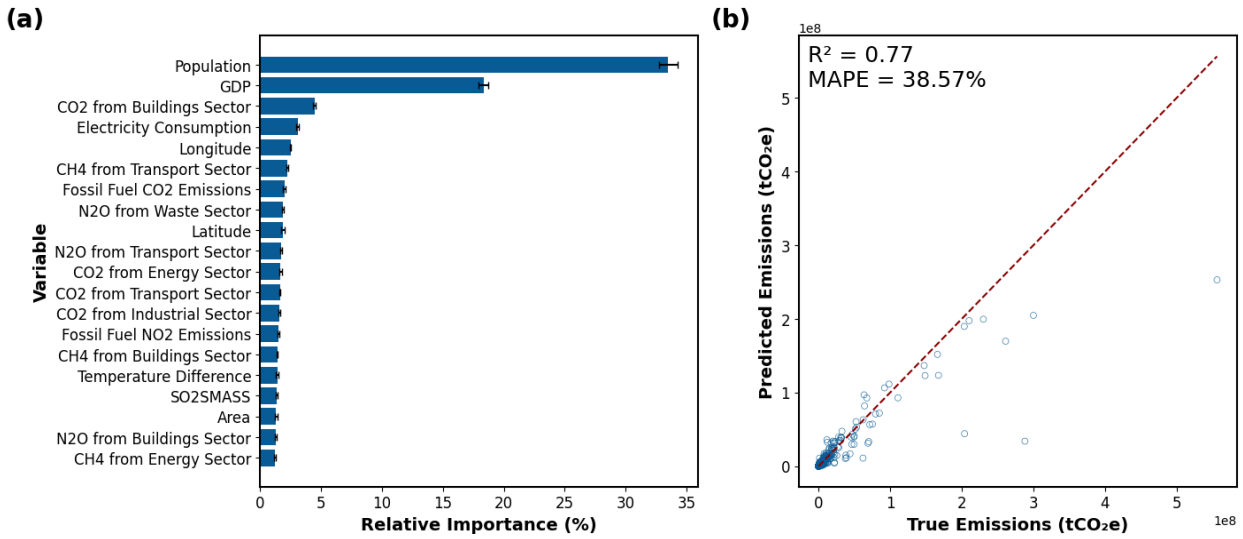

Figure 4. a) Feature importance describing which variables contribute to the overall machine learning model's performance; and b) model performance (R^2 and MAPE) comparing the self-reported emissions data and the final predicted CO_2eq emissions of subnational units. The error bar presents uncertainty bound due to feature shuffling. Performance metrics are calculated based on the original scale.

We benchmark AutoGluon against the widely used traditional machine learning model XGBoost, used in Hsu et al. (2022)[17] to evaluate its relative performance in handling high-dimensional features. As shown in Supplementary Table S2, AutoGluon outperforms XGBoost in both model predictive accuracy and generalization capability, motivating our selection of AutoGluon as the primary predictive model. The final trained model is used to generate subnational-level CO_2eq emissions estimates from 2000 to 2020, producing a consistent emissions dataset.

Data limitations

Our dataset and model is limited by several constraints. First, most of the data are self-reported by subnational actors that participate in international climate initiatives, although some of the data are derived from national-level efforts (e.g., the China Carbon Neutrality Tracker, see Table S1). While there are most certainly subnational entities outside of these initiatives pledging climate actions and reporting emission inventories, we are unable to systematically capture and assess them due to the unwieldy nature and infeasibility of collecting every instance outside of common networks and reporting platforms. Second, due to the nature of our spatial standardization, we are unable to include entities that have no available spatial boundaries (e.g., municipal corporations, regional cooperative associations, or associations of municipalities). Although in some cases we were able to use Open Street Maps to identify an alternative spatial boundary, in some cases no authoritative data sources were available to validate this information. Finally, the availability of Global South data is still a major limitation for the scope of the study. Specifically, we could only find 628 self-reported emissions data points for cities and regions outside of the G20, and we could only identify geographic boundaries for 265, either due to

unavailable geometries or by insufficient information on the data sources to unequivocally identify the entity's geometry.

Another aspect to consider is the differences in the way that subnational governments report their GHG emissions and the scopes, sectors and GHG they consider in their inventories. Supplementary Figure S1 shows the differences in GHG coverage in self-reported emissions data from G20 countries by regions (i.e., whether a subnational entity reports only CO_2 emissions or also additional GHG gases such as CH_4, N_2O and F-gases in CO_2eq). Subnational entities in Europe and Eastern Europe and Central Asia regions show over 60% of self-reported emissions covering CO_2 and other GHG gases, with fewer than 20% providing insufficient information to evaluate the GHG coverage. On the contrary, other global regions show close to 50% of self-reported emissions data with insufficient information to unequivocally identify their GHG coverage even when the emissions units are CO_2eq. While we have not considered global regions or countries as predictors to reduce regional overfitting, these inconsistencies in the self-reported subnational emission data could still be a source of bias, particularly outside of Europe, where some of the predicted results could be underestimated due to the inherent characteristics of the training data for countries in those areas.

Data Records

We provide model-predicted CO_2 e emissions data for G20 subnationals (refer to Supplementary Figure S2 for which GADM levels are available by country) from 2000 to 2020. Each row in the CSV file represents a specific administrative unit in a given year. The variables included are:

- WB_region: One of eight World Bank geographic regions (North America, Latin America and the Caribbean, East Asia and the Pacific, Europe, Eastern Europe and Central Asia, Sub-Saharan Africa, and South Asia)
- ISO: The ISO 3166-1 alpha-3 country codes (e.g., USA for the United States of America)
- Country: Name of the country that includes the subnational unit
- Region: The highest administrative level (typically admin_1) containing the observation (e.g., "State of New York" is the state-level administrative name for the unit "County of Albany, NY")
- Name_full: Human-readable name of the subnational unit, standardized for clarity and consistency (aligned with the ClimActor naming conventions, see Hsu et al., 2020) (e.g., "County of Albany, NY")
- Name_short: Simplified Name_full (e.g., "Albany" is short for "County of Albany, NY")
- Year: Calendar year of the emissions estimate.
- Pred_emissions: Predicted annual CO2eq emissions (in metric tons) for the administrative unit based on our model.
- lat: Latitude of the administrative unit geometry's centroid.

- long: Longitude of the administrative unit geometry's centroid.

The model-predicted CO_2eq emissions data are available for download from [link].

Data Examples

Predicted changes in greenhouse gas emissions at the subnational level reflect the geographic, economic and developmental trajectories of regions within the world's largest economies. Figure 5 shows the percent change in predicted emissions between 2000 and 2020 across administrative level 1 units (e.g., states or provinces) in G20 countries. Regions in parts of North America and Europe exhibit emission declines, notably several US states including the District of Columbia (38%) and Maryland (35%), and some areas in Europe such as Bulgaria's Province of Vratsai (31%) or Greece's Epirus and Western Macedonia (35%) show marked emission declines over the 20-year period. In contrast, rapid emission increases are evident across much of Turkey, India, China, Southeast Asia and South America such as Turkey's Province of Denizli that saw an increase of over 300% or India's State of Sikkim that increased emissions by 220% in the same period. At a national level, we also find consistency in emissions reduction trends, as in the case of the US, we observe a 16.3% reduction in aggregate emissions from 5,422.584 $MTCO_2$ in 2005 to 4,536.724 $MTCO_2$ in 2020 -- consistent with official U.S. Environmental Protection Agency reports.[43] On the contrary, China has seen an increase of 91% for the whole period and 28% for the period between 2005 and 2010, which is consistent with the 31% increase reported in total CO_2eq emissions through their nationally determined contribution (NDC).[44]

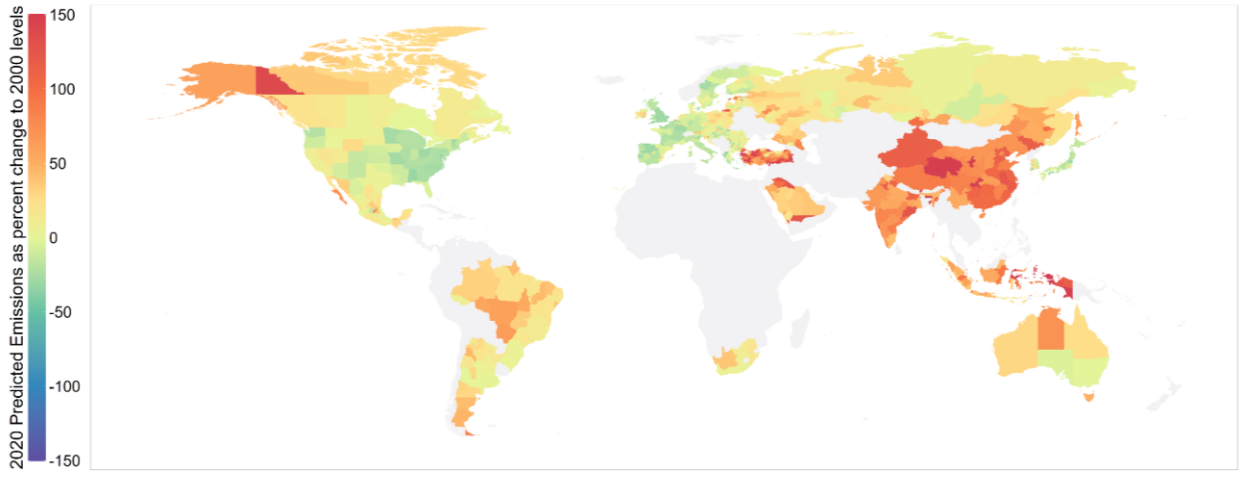

Figure 5. Percentage change of predicted greenhouse gas emissions between 2000 and 2020 for administrative level 1 of G-20 countries.

Examining more closely into individual countries and finer-scale geographic units allow for insight into the spatial distribution of greenhouse gas emissions within countries. Figure 6

showcases three selected countries: France, Canada, and South Africa and illustrates how greenhouse gas emissions vary across administrative levels within these countries, offering insights into which subnational areas may be driving greenhouse gas emissions. The maps of France and South Africa show that while total emissions at the administrative level 1 are relatively similar; when examining emissions at administrative level 2 and 3, it becomes clear that states and provinces containing major cities are primary emitters. In Canada, the high emissions are mainly observed in major cities located in Ontario and Quebec showing consistency with the country's population and GDP centers. Although not densely populated, several administrative level 3 units in the Alberta region also contribute a significant amount of greenhouse gas emissions due to local oil and gas industries.

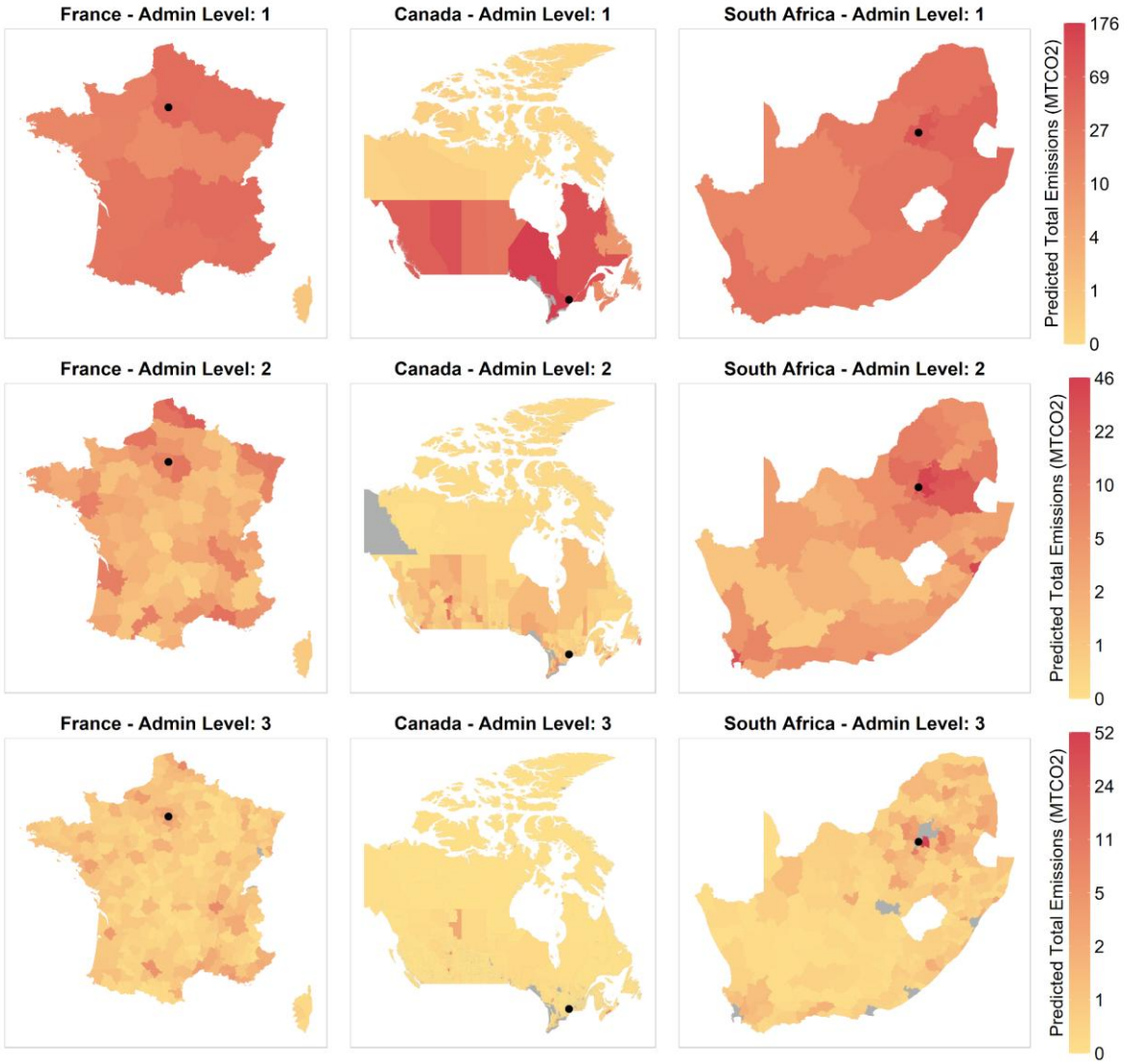

Figure 6. Predicted emissions in 2020 at the administrative level 1-3 for selected countries. Note: The black dots represent the representative cities of the selected counties, namely Paris, Ottawa, and Johannesburg from left to right.

Examining temporal trends in predicted emissions for selected urban and regional areas reveals further heterogeneity in emission trajectories and underlying drivers. As shown in Figure 7, many cities exhibit diverging emission paths over time. Lombardy, a region in Italy, shows dramatic declining emissions, most likely due to its decline in territorial emissions (panel B). Changwon (Korea), Johannesburg (South Africa), Ekurhuleni (South Africa), and Buenos Aires (Brazil) show relative stable emissions except for the year or so leading up to 2020, driving consistently by population (panel C), GDP (panel D) and electricity consumption growth (panel E), despite estimated declines in territorial CO_2 emissions (panel B). These patterns reflect the differences in socioeconomic development and energy use that drive varying trends in predicted emissions, highlighting their relevance as key predictors. While we see consistent temporal patterns between predicted emissions and underlying predictors, we also observe higher values of predicted CO_2e emissions compared to territorial CO_2eq emissions, for example, in the case of Buenos Aires in Figure 7. This difference, also noted in Figure 3, highlights the difficulties of accurately estimating emissions using gridded datasets, particularly in smaller geometries especially when high-emitting facilities are located outside or near the boundaries of the administrative entities.

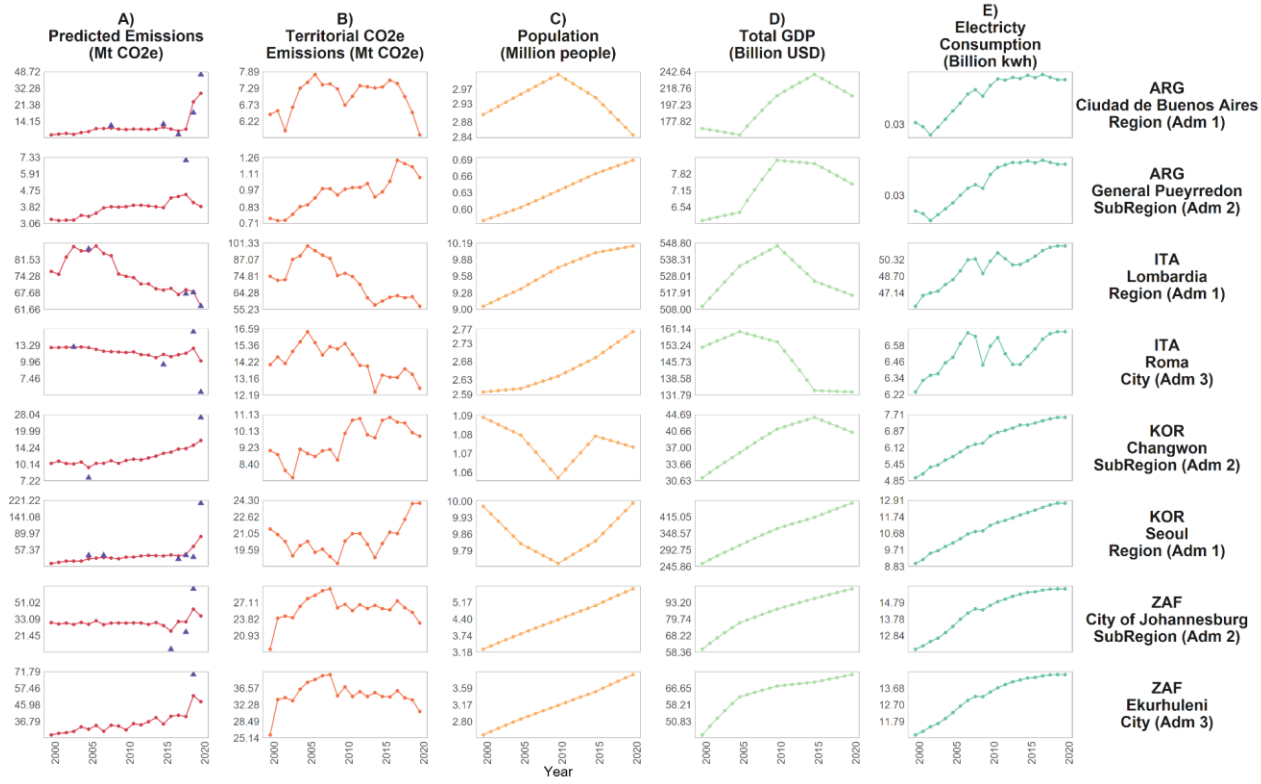

Figure 7. Plot of predicted emissions and selected underlying predictors used, including EDGAR CO_2 emissions, population, total GDP, and electricity consumption for selected cities from 2000–2020. The triangles (▲) in panel A represent self-reported emissions inventories.

Technical Validation

Due to the scarcity of publicly available, self-reported subnational greenhouse gas inventories, there is no comprehensive external validation dataset against which we can fully assess our model. In fact, our framework effectively represents, to our knowledge, the most comprehensive subnational emissions dataset for the G20 currently available, and it can be readily scaled to other countries and globally. Therefore, to evaluate the plausibility and performance of our predictions, we instead compare our estimates to alternative city-level emissions datasets derived from two major methodological approaches: statistically down-scaled emissions from the Global Covenant of Mayors for Climate and Energy (GCoM) Data Portal for Cities (abbreviated hereafter as DPfC) and the Global Gridded Daily CO2 Emissions Dataset (GRACED) database.

Validation against other datasets

The DPfC dataset, developed by the World Resources Institute (WRI) and GCoM, provides city-scale greenhouse gas emissions estimates using the Common Reporting Framework (CFM). The dataset uses sector-specific and statistical downscaling methodologies to estimate emissions across various sectors, such as buildings and stationary energy, transportation and mobile energy, and waste. These estimates are derived through a combination of national and regional statistics, and the local contextual information. Emission factors are also adjusted to align with specific municipal boundaries. Emissions from Industrial Processes and Product Use (IPPU) and Agriculture, Forestry and Other Land Use (AFOLU) are not required by this framework but are reported by some countries.[45]

As of June 2025, we downloaded available data for G20 countries, including Brazil, Canada, Denmark, Indonesia, India, Japan, Mexico, and the United States. Each of these countries contains at least one year of emission data from 2000 to 2020, allowing for comparative analysis with our model results. In most countries, IPPU emissions are not available, and emissions from AFOLU are excluded from our comparison analysis to make it consistent with the scope of sectors in our self-reported emission dataset.

Figure 8 shows the comparison results for each country between our model's predicted emissions and the DPfC data for Brazil, Canada, Denmark, and Japan. Overall, our predictions are higher than the DPfC emissions estimates, as demonstrated through Figure 8, which shows that for most countries our estimated greenhouse gas emissions values are above the parity line. Denmark, Canada and Mexico are the only countries where we found a R^2 value over 0.5, indicating a relatively strong relationship between our prediction and the DPfC dataset. In Denmark and Mexico, the regression slopes are close to 1, indicating that the variation in the emissions is captured. The poor model fit ($R^2 = 0$) in the remaining countries does not support a reliable interpretation of the regression parameters. However, a pattern of slopes greater than 1 and with most predicted emissions above the parity line is observed in countries such as Brazil, Japan,

Indonesia, and the United States. This trend suggests a systematic offset between the two datasets, with our predicted emissions typically higher than the DPfC emissions. One possible explanation for these discrepancies is that almost all actors from the DpfC do not include IPPU emissions: for example, fewer than 1% of Brazilian cities report IPPU data. Additionally, transportation sector emission data is not available for actors from Indonesia, India, and Japan, nor does their data documentation include the specifications for these two sectors. These sector differences likely result in a significant underestimation of actor annual emissions in the DPfC dataset.

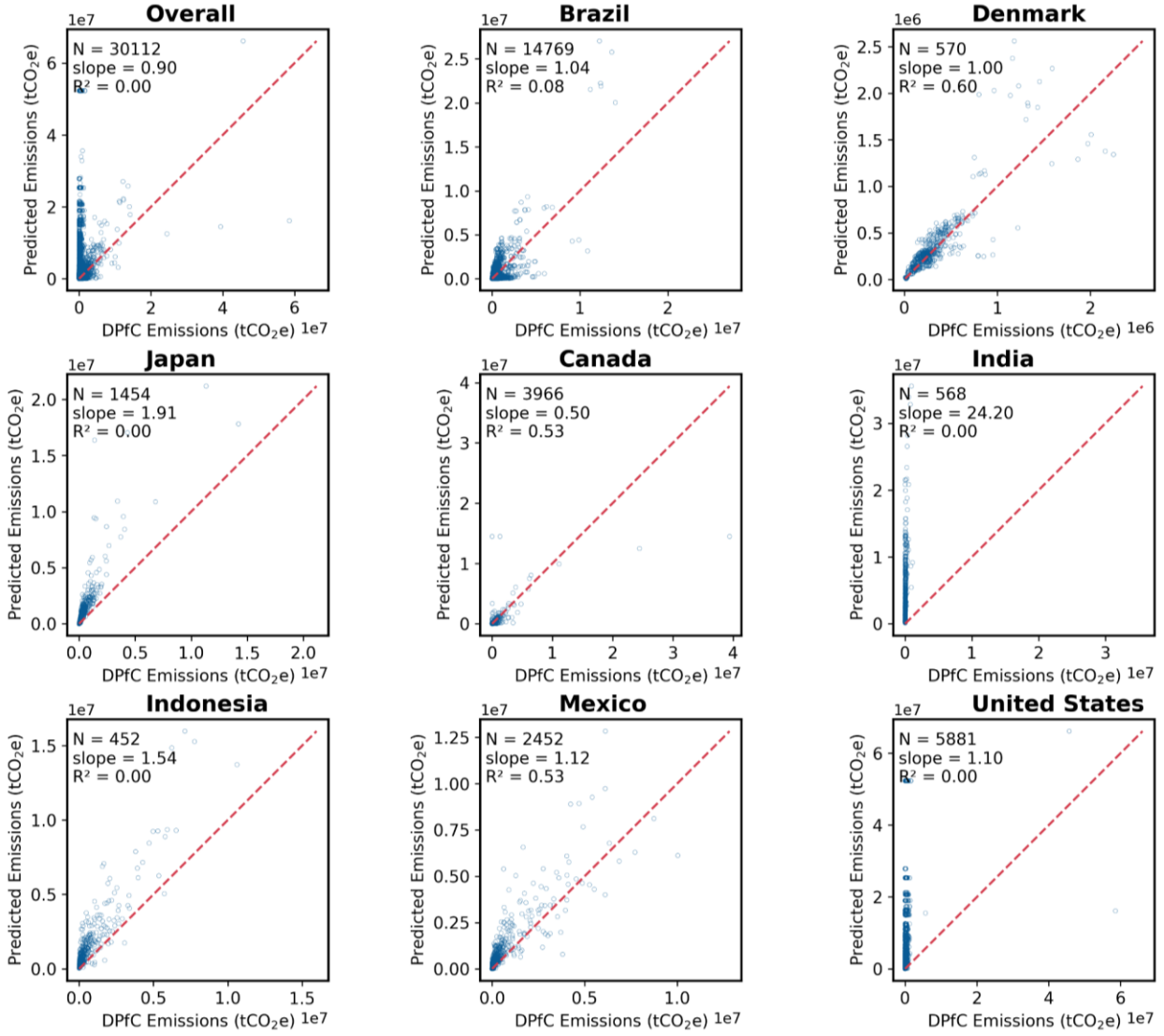

Figure 8. Comparison of annual emissions for subnational actors: Model predicted emissions vs. Data Portal for Cities (abbreviated as DPfC).

In addition, we extracted CO_2 emission data for G20 countries from the GRACED dataset, which provides $0.1° \times 0.1°$ gridded emissions at a daily resolution from cement production and fossil fuel combustion across major sectors (industry, power, residential, ground transportation,

international aviation, domestic aviation, and international shipping).[46] We compared our model-predicted self-reported emissions with GRACED data across multiple administrative levels to evaluate our predictions (Figure 9). The comparison shows strong overall consistency, with a coefficient of determination (R^2) of 0.82 for the full sample and the highest consistency at administrative level 1 ($R^2 = 0.87$). We also find that consistency decreases at finer administrative levels, reflecting increasing discrepancies at subnational scales. These differences may partly stem from the ~20% uncertainties reported in GRACED estimates and, more importantly, highlight the challenges of reconciling emission estimates at city or finer administrative levels. In addition, GRACED reports only CO_2 emissions, whereas our self-reported predictions are based on CO2-equivalent (CO_2eq), which inherently yields higher values and may further contribute to these discrepancies.

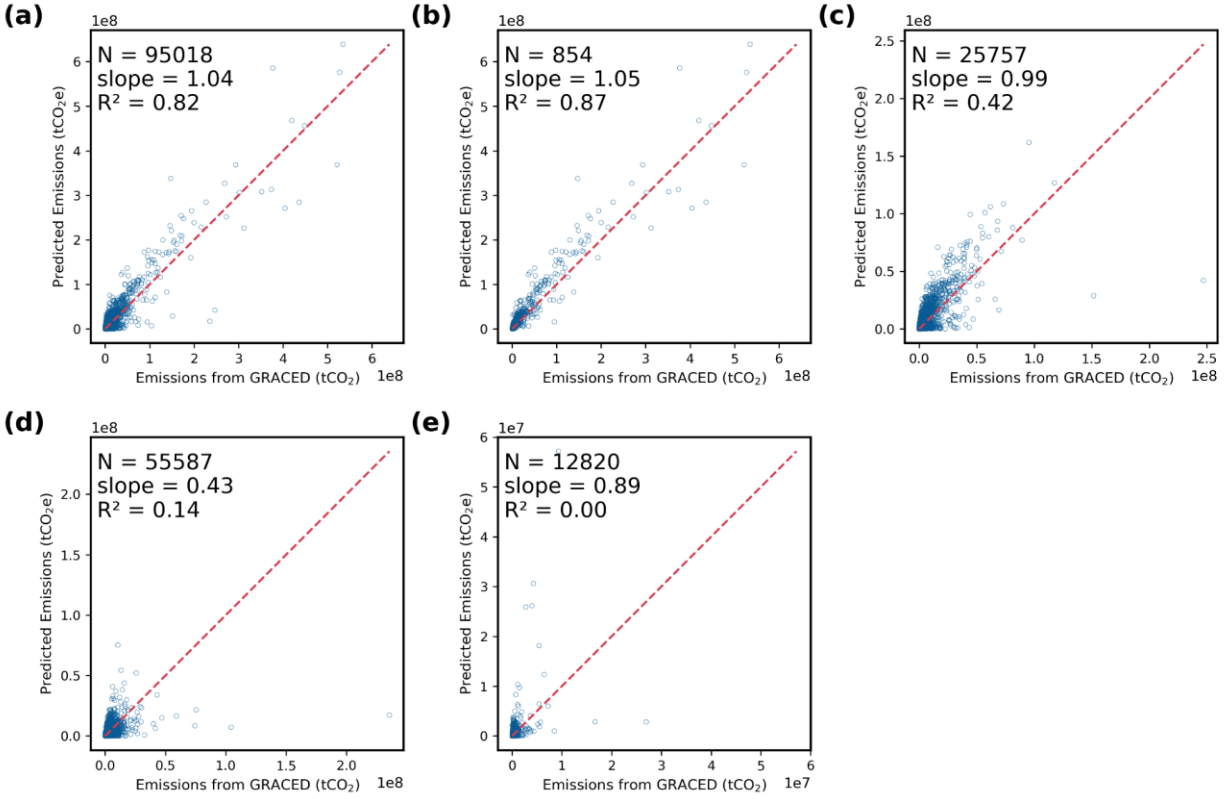

Figure 9. Comparison between model predicted emissions v.s. GRACED emissions in 2019. Note: (a) all administrative levels; (b) administrative level 1; (c) administrative level 2; (d) administrative level 3; (e) administrative level 4.

Uncertainty Analysis

We quantify the variability in feature contributions during training using the 99th percentile bounds (p99_low and p99_high) from repeated permutations of feature importance (Figure 4). These bounds provide an empirical estimate of the uncertainty associated with the relative importance of each feature. The generally narrow ranges across most features indicate consistent attribution of predictive influence.

Usage Notes

Predicted results should be considered the total yearly CO_2eq emissions for Scope 1+2 for Building, Energy, Industrial, Waste and Ground Transportation sectors for the corresponding year. Emissions are reported at multiple subnational administrative levels within G20 countries. Users are provided with both time series prediction results for all G20 administrative units as well as the trained machine learning model product, which can be used to generate emissions predictions for other areas of interest within G20 countries. Model inputs should be transformed using Hyperbolic arcsine transformation and output is generated under the same transformation, predicted values at tons of CO_2 equivalent (tCO_2e) are obtained by using inverse hyperbolic arcsine.

It is important to emphasize that these predicted emissions estimates are not intended to replace official or locally produced greenhouse gas inventories by subnational governments themselves. Rather, they serve as a supplemental data product designed to provide consistent, spatially complete estimates that enable time series analyses, identification of emission hotspots, and integration into climate impact or mitigation scenario modelling. For cities or regions with limited technical or institutional capacity to produce high-quality inventories, these estimates may provide a useful baseline or diagnostic starting point.

As demonstrated in our data comparison with other city-level emission datasets, such as the GCoM Data Portal for Cities or GRACED, the dataset described in this paper offers the advantage of being fully consistent across space and time while still aligning to administrative boundaries relevant for policy and governance. In particular, compared to these other datasets, the data provided in this study is better able to accurately capture smaller administrative subnational units' emissions. While gridded products are useful for global comparability, they often do not conform to subnational jurisdictions, limiting their relevance for local decision-making. Conversely, our model is specifically designed to work at the administrative level, making it more suitable for understanding subnational trends and informing city or regional climate planning.

Code Availability

Machine learning and plotting were performed using Python and R. The final trained machine learning model, data, and materials are publicly available via [link].

Acknowledgements

The authors thank Noah Civiletti, Emma Holmes, and Izzy Bukovnik for assistance in data extraction. This work was funded by an IKEA Foundation (Grant no. G-2306-02289) and the National Science Foundation (Grant no. 2216592) to A. Hsu.

Author Contributions

Y.Y., X.W., and D.M. contributed equally to the study. Y.Y., X.W., and D.M. collected data and conducted the analysis. X.W., D.M., and A.H. cleaned and compiled the data. Y.Y. and X.W. contributed to the method. A.H. conceptualized and supervised the study. Y.Y., X.W., D.M., and A.H. wrote the manuscript. All coauthors reviewed, edited, and approved the manuscript.

Competing Interests

The authors declare no competing interests.

References

1. UNFCCC. Global Climate Action Portal. https://climateaction.unfccc.int/ (2025).
2. Net Zero Tracker. Net Zero Tracker. https://zerotracker.net/ (2025).
3. Song, K., Burley Farr, K. & Hsu, A. Assessing subnational climate action in G20 cities and regions: Progress and ambition. *One Earth* **7**, 2189–2203 (2024).
4. Ibrahim, N., Sugar, L., Hoornweg, D. & Kennedy, C. Greenhouse gas emissions from cities: comparison of international inventory frameworks. *Local Environ.* **17**, 223–241 (2012).
5. Marcotullio, P., Sarzynski, A., Albrecht, J., Schulz, N. & Garcia, J. Assessing urban greenhouse gas emissions in European medium and large cities: Methodological considerations. (2016).
6. Gurney, K. R. *et al.* Under-reporting of greenhouse gas emissions in U.S. cities. *Nat. Commun.* **12**, 553 (2021).
7. Crippa, M. *et al.* Insights into the spatial distribution of global, national, and subnational greenhouse gas emissions in the Emissions Database for Global Atmospheric Research (EDGAR v8. 0). *Earth Syst. Sci. Data* **16**, 2811–2830 (2024).
8. Kuriakose, J., Jones, C., Anderson, K., McLachlan, C. & Broderick, J. What does the Paris climate change agreement mean for local policy? Downscaling the remaining global carbon budget to sub-national areas. *Renew. Sustain. Energy Transit.* **2**, 100030 (2022).
9. Huo, D. *et al.* Carbon Monitor Cities near-real-time daily estimates of CO2 emissions from 1500 cities worldwide. *Sci. Data* **9**, 533 (2022).
10. Moran, D. *et al.* Carbon footprints of 13 000 cities. *Environ. Res. Lett.* **13**, 064041 (2018).

11. Moran, D. *et al.* Estimating CO2emissions for 108000 European cities. *Earth Syst. Sci. Data* **14**, 845–864 (2022).
12. Yu, Y., Manya, D. & Hsu, A. Bridging Territorial and Consumption-Based Emissions for Urban Climate Action Assessment. *Eartharxiv preprint* (2025). doi:10.31223/X5PB02.
13. Jin, Y. & Sharifi, A. Machine learning for predicting urban greenhouse gas emissions: A systematic literature review. *Renew. Sustain. Energy Rev.* **215**, 115625 (2025).
14. Dodman, D. Forces driving urban greenhouse gas emissions. *Curr. Opin. Environ. Sustain.* **3**, 121–125 (2011).
15. Marcotullio, P. J., Sarzynski, A., Albrecht, J., Schulz, N. & Garcia, J. The geography of global urban greenhouse gas emissions: an exploratory analysis. *Clim. Change* **121**, 621–634 (2013).
16. Dodman, D. *et al.* Cities, Settlements and Key Infrastructure. in *Climate Change 2022: Impacts, Adaptation and Vulnerability. Contribution of Working Group II to the Sixth Assessment Report of the Intergovernmental Panel on Climate Change* (eds. Pörtner, H.-O. et al.) 907–1040 (Cambridge University Press, Cambridge, UK and New York, NY, USA, 2022). doi:10.1017/9781009325844.008.
17. Hsu, A., Wang, X., Tan, J., Toh, W. & Goyal, N. Predicting European cities' climate mitigation performance using machine learning. *Nat. Commun.* **13**, 7487 (2022).
18. Chen, T. & Guestrin, C. XGBoost: A scalable tree boosting system. in *Proceedings of the ACM SIGKDD International Conference on Knowledge Discovery and Data Mining* vols 13-17-Augu 785–794 (ACM, 2016).
19. Feng, W. *et al.* Application of Neural Networks on Carbon Emission Prediction: A Systematic Review and Comparison. *Energies* **17**, 1628 (2024).
20. Lwasa, S. *et al.* Urban systems and other settlements. in *Climate Change 2022: Mitigation of Climate Change. Contribution of Working Group III to the Sixth Assessment Report of the Intergovernmental Panel on Climate Change* (eds. Shukla, P. R. et al.) 861–952 (Cambridge University Press, Cambridge, UK and New York, NY, USA, 2022). doi:10.1017/9781009157926.010.

21. GADM. Database of Global Administrative Areas. (2024).
22. UNEP. *Emissions Gap Report 2024: No More Hot Air ... Please!* https://unepccc.org/emissions-gap-reports/ (2024).
23. Hsu, A. *et al.* ClimActor, harmonized transnational data on climate network participation by city and regional governments. *Sci. Data* **7**, 374–374 (2020).
24. IPCC. *Climate Change 2022: Mitigation of Climate Change. Contribution of Working Group III to the Sixth Assessment Report of the Intergovernmental Panel on Climate Change*. (Cambridge University Press, Cambridge, UK and New York, NY, USA, 2022). doi:10.1017/9781009157926.
25. Kona, A. *et al.* Global Covenant of Mayors, a dataset of greenhouse gas emissions for 6200 cities in Europe and the Southern Mediterranean countries. *Earth Syst. Sci. Data* **13**, 3551–3564 (2021).
26. Data Driven Yale, NewClimate Institute, & PBL Environmental Assessment Agency. *Global Climate Action from Cities, Regions, and Businesses: Individual Actors, Collective Initiatives and Their Impact on Global Greenhouse Gas Emissions*. https://datadrivenlab.org/wp-content/uploads/2018/08/YALE-NCI-PBL_Global_climate_action.pdf (2018).
27. World Bank. Total greenhouse gas emissions excluding LULUCF per capita. (2023).
28. Oda, T., Maksyutov, S. & Andres, R. J. The Open-source Data Inventory for Anthropogenic CO_2 , version 2016 (ODIAC2016): a global monthly fossil fuel CO_2 gridded emissions data product for tracer transport simulations and surface flux inversions. *Earth Syst. Sci. Data* **10**, 87–107 (2018).
29. Spinoni, J. *et al.* Changes of heating and cooling degree-days in Europe from 1981 to 2100. *Int. J. Climatol.* **38**, e191–e208 (2018).
30. Engel-Cox, J., Kim Oanh, N. T., van Donkelaar, A., Martin, R. V. & Zell, E. Toward the next generation of air quality monitoring: Particulate Matter. *Atmos. Environ.* **80**, 584–590 (2013).
31. van Donkelaar, A. *et al.* Monthly Global Estimates of Fine Particulate Matter and Their Uncertainty. *Environ. Sci. Technol.* **55**, 15287–15300 (2021).
32. Hammer, M. S. *et al.* Assessment of the impact of discontinuity in satellite instruments and retrievals on global PM2.5 estimates. *Remote Sens. Environ.* **294**, 113624 (2023).

33. Cooper, M. J. *et al.* Global fine-scale changes in ambient NO2 during COVID-19 lockdowns. *Nature* **601**, 380–387 (2022).
34. Global Modeling And Assimilation Office & Pawson, S. MERRA-2 tavgM_2d_aer_Nx: 2d,Monthly mean,Time-averaged,Single-Level,Assimilation,Aerosol Diagnostics V5.12.4. NASA Goddard Earth Sciences Data and Information Services Center https://doi.org/10.5067/FH9A0MLJPC7N (2015).
35. Qi, L. & Wang, S. Fossil fuel combustion and biomass burning sources of global black carbon from GEOS-Chem simulation and carbon isotope measurements. *Atmospheric Chem. Phys.* **19**, 11545–11557 (2019).
36. Stanelle, T., Bey, I., Raddatz, T., Reick, C. & Tegen, I. Anthropogenically induced changes in twentieth century mineral dust burden and the associated impact on radiative forcing. *J. Geophys. Res. Atmospheres* **119**, 13,526-13,546 (2014).
37. Chen, J. *et al.* Global 1 km\times 1 km gridded revised real gross domestic product and electricity consumption during 1992–2019 based on calibrated nighttime light data. *Sci. Data* **9**, 202 (2022).
38. Schiavina, M., Melchiorri, M. & Freire, S. GHS-DUC R2023A - GHS Degree of Urbanisation Classification, application of the Degree of Urbanisation methodology (stage II) to GADM 4.1 layer, multitemporal (1975-2030). European Commission, Joint Research Centre (JRC) https://doi.org/10.2905/DC0EB21D-472C-4F5A-8846-823C50836305 (2023).
39. Kummu, M., Kosonen, M. & Masoumzadeh Sayyar, S. Downscaled gridded global dataset for gross domestic product (GDP) per capita PPP over 1990–2022. *Sci. Data* **12**, 178 (2025).
40. Perry, M. rasterstats. (2021).
41. Yu, Y., Li, X., Hsu, A. & Kittner, N. Mapping Spatiotemporal Disparities in Residential Electricity Inequality Using Machine Learning. *Environ. Sci. Technol.* **58**, 19999–20008 (2024).
42. Erickson, N. *et al.* AutoGluon-Tabular: Robust and Accurate AutoML for Structured Data. Preprint at https://doi.org/10.48550/arXiv.2003.06505 (2020).
43. EPA. *Inventory of U.S. Greenhouse Gas Emissions and Sinks: 1990-2022*. https://www.epa.gov/ghgemissions/inventory-us-greenhouse-gas-emissions-and- sinks-1990-2022.

(2024).

44. UNFCCC. GHG data from UNFCCC. *GHG data from UNFCCC* https://unfccc.int/topics/mitigation/resources/registry-and-data/ghg-data-from-unfccc (2025).
45. Global Covenant of Mayors for Climate & Energy. Data Portal for Cities. http://www.dataportalforcities.org (2025).
46. Dou, X. *et al.* Near-real-time global gridded daily CO2 emissions 2021. *Sci. Data* **10**, 69 (2023).